PHYSICAL REVIEW VOLUME 148, NUMBER 1 5 AUGUST 1966

Wick and Goldstone Theorems for General Spin; Antiferromagnetic Spin Waves. II*

YUNG-LI WANG AND H. B. CALLEN
Department of Physics, University of Pennsylvania, Philadelphia, Pennsylvania
(Received 13 January 1966)

The analogs of Wick's theorem and of Goldstone's theorem, proved in a previous paper for spin $\frac{1}{2}$, are generalized to arbitrary spin. The proof is based on the Schwinger coupled-boson representation of spin operators. Quantum corrections to the spin-wave modes in antiferromagnets are again considered, and it is shown that these corrections can be expanded in powers of $1/2Sz$, where z is the number of nearest neighbors. For large S the $1/S$ factor presumably provides convergence, as assumed by Oguchi, whereas for $S=\frac{1}{2}$ the expansion parameter reduces to $1/z$, as discussed in the preceding paper.

1. INTRODUCTION

In the preceding paper,[1] to be referred to as I, we have derived a particular form of Wick theorem and a Goldstone linked-diagram expansion theorem, for spin $\frac{1}{2}$. The utility of those theorems was demonstrated by calculation of the leading quantum corrections to simple spin waves in antiferromagnets. In this paper we generalize the results to arbitrary spin.

The method used in this paper is quite different from that of I, and it may appeal to many readers as more transparent despite (or perhaps because of) its greater generality. In I the Wick-like theorem was discussed directly in terms of spin-$\frac{1}{2}$ operators, although we have also given[2] an equivalent proof using the coupled-fermion representation of spin-$\frac{1}{2}$ operators. We here introduce Schwinger's coupled-boson representation of general spin operators,[3] permitting the use of standard theorems for boson operators. Our proof is closely related to one given by Davis,[4] although the forms of the final theorems are quite different.

In the application made in I we derived the dominant quantum corrections to the spin waves in antiferromagnets. For spin $\frac{1}{2}$ it was found that these corrections represented the leading terms in a series in $1/z$, where z is the number of nearest neighbors. We here briefly reconsider the same problem for arbitrary spin, and we find that the corresponding expansion parameter is $1/2zS$. This makes contact both with I and with the conventional Oguchi expansion in powers of $1/S$.[5]

2. WICK'S THEOREM

Following Schwinger[3,4] we introduce the operators u_i, $u_i^\dagger$ and v_i, $v_i^\dagger$ at the ith site by

$$S_i^+=v_i^\dagger u_i\,, \tag{1}$$

$$S_i^-=u_i^\dagger v_i\,, \tag{2}$$

$$S_i^z=\tfrac{1}{2}(v_i^\dagger v_i-u_i^\dagger u_i)=v_i^\dagger v_i-S\,, \tag{3}$$

where the last equality follows from the auxiliary constraint [equivalent to the condition $\mathbf{S}_i\cdot\mathbf{S}_i=S(S+1)$],

$$v_i^\dagger v_i+u_i^\dagger u_i=2S\,. \tag{4}$$

The commutation relations of the spin operators imply that the u particles and v particles are conventional bosons:

$$[u_i,u_j^\dagger]=[v_i,v_j^\dagger]=\delta_{ij}\,, \tag{5}$$

$$[u_i,u_j]=[v_i,v_j]=0\,, \tag{6}$$

and

$$[u_i,v_j^\dagger]=[u_i,v_j]=0\,. \tag{7}$$

It is convenient to define an unperturbed Hamiltonian by

$$\mathcal{H}_0=\sum_i \omega_{0i}S_i^z\,. \tag{8}$$

Here, ω_{0i} will be taken as independent of the site index i for a ferromagnet, whereas in the antiferromagnet we will take $\omega_{0i}=\pm\omega_0$ according to the sublattice of the site i. Consequently the unperturbed ground state $|0\rangle$ is the state in which the spin i is down if ω_{0i} is positive, or up if ω_{0i} is negative.

Writing

$$\mathcal{H}=\mathcal{H}_0+V\,, \tag{9}$$

the relation between an operator $O(t)$ in interaction representation, O_s in Schrödinger representation, and $O_H(t)$ in Heisenberg representation, is

$$O(t)=e^{i\mathcal{H}_0t}O_se^{-i\mathcal{H}_0t}=\mathcal{S}(t)O_H(t)\mathcal{S}^{-1}(t)\,, \tag{10}$$

where

$$\mathcal{S}(t)=P\exp\left(-i\int_{-\infty}^{t}V(t')dt'\right). \tag{11}$$

In particular,

$$S_i^\pm(t)=e^{\pm i\omega_{0i}t}S_i^\pm\,. \tag{12}$$

---

* Supported by the Office of Naval Research. This work is a contribution of the Laboratory for Research on the Structure of Matter of the University of Pennsylvania.

[1] Y. L. Wang, S. Shtrikman, and H. B. Callen, preceding paper, Phys. Rev. **148**, 419 (1966).

[2] Y. L. Wang, S. Shtrikman, and H. B. Callen, J. Appl. Phys. **37**, 1451 (1966).

[3] J. Schwinger, Atomic Energy Commission Report No. NYO-3071, 1952 (unpublished). See also D. Mattis, *The Theory of Magnetism* (Harper and Row, New York, 1965).

[4] H. L. Davis, Phys. Rev. **120**, 789 (1960).

[5] T. Oguchi, Phys. Rev. **117**, 117 (1960).

In the coupled-boson representation the ground state for the ith spin (assumed down for definiteness) contains no v particles but contains $2S$ u particles. That is,

$$|0\rangle_i=[(2S)!]^{-1/2}(u_i^+)^{2S}\|0\rangle\,, \tag{13}$$

where $\|0\rangle$ designates the "boson-vacuum state"

$$u_i\|0\rangle=v_i\|0\rangle=0\,. \tag{14}$$

If the ground state of the ith spin is up ($\omega_{0i}<0$) the $u_i^\dagger$ operators in Eq. (12) are replaced by $v_i^\dagger$ operators.

The unperturbed Hamiltonian (8) becomes

$$\mathcal{H}_0=-S\sum_i \omega_{0i}+\sum_i \omega_{0i}v_i^\dagger v_i\,, \tag{15}$$

whence

$$v_i^\dagger(t)=e^{i\omega_{0i}t}v_i^\dagger\,, \tag{16}$$

$$v_i(t)=e^{-i\omega_{0i}t}v_i\,, \tag{17}$$

$$u_i^\dagger(t)=u_i^\dagger\,, \tag{18}$$

and

$$u_i(t)=u_i\,. \tag{19}$$

Consider now the chronological product

$$\mathcal{G}\equiv\langle 0|PS_1^-S_2^-\cdots S_\alpha^-S_{1'}^+S_{2'}^+\cdots S_{\alpha'}^+|0\rangle\,, \tag{20}$$

where the subscripts on $S^\pm$ are now to be understood as denoting both a site index and a time, and where P is the Dyson time-ordering operator which simply arranges factors in increasing time sequence from right to left. In terms of the coupled bosons we have

$$\mathcal{G}=\langle 0|Pu_1^\dagger v_1u_2^\dagger v_2\cdots u_\alpha^\dagger v_\alpha v_{1'}^\dagger \times u_{1'}v_{2'}^\dagger u_{2'}\cdots v_{\alpha'}^\dagger u_{\alpha'}|0\rangle \tag{21}$$

$$=\langle 0|Pv_1v_2\cdots v_\alpha v_{1'}^\dagger v_{2'}^\dagger\cdots v_{\alpha'}^\dagger|0\rangle \times\langle 0|Pu_1^\dagger u_2^\dagger\cdots u_\alpha^\dagger u_{1'}u_{2'}\cdots u_{\alpha'}|0\rangle\,. \tag{22}$$

We now apply the standard form of Wick's theorem to the v factor in Eq. (22) (but not to the u factor).[6] The v factor becomes the sum of products of factors of the form $\langle 0|Pv_iv_j^\dagger|0\rangle$, corresponding to all possible sets of complete contractions. Denoting the u factor by $u_{12\cdots\alpha}$ we then have

$$\mathcal{G}=\sum_{\text{contractions}}\{\langle 0|Pv_iv_j^\dagger|0\rangle\langle 0|Pv_lv_m^\dagger|0\rangle\cdots\}u_{12\cdots\alpha}\,. \tag{23}$$

Noting also that

$$\langle 0|Pv_iv_j^\dagger|0\rangle=(1/2S)\langle 0|PS_i^-S_j^+|0\rangle\,, \tag{24}$$

we can write

$$\mathcal{G}=\sum_{\text{contractions}}\{\langle 0|PS_i^-S_j^+|0\rangle \times\langle 0|PS_l^-S_m^+|0\rangle\cdots\}u_{12\cdots\alpha}/(2S)^\alpha\,. \tag{25}$$

[6] Recalling Eq. (13) one can also decompose the factor by Wick's theorem. The contractions then involve the u operators implicitly introduced by (13) as well as those explicitly appearing in (22). Summation of all u-particle diagrams would then be required to achieve our results. Davis (Ref. 4) on the other hand, performs a Wick-decomposition of the explicit u operators only.

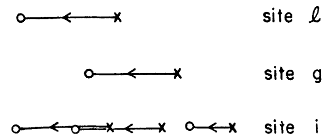

FIG. 1. A typical diagram for a chronological product. The u factor is the product of $(2S)$ from site l, $(2S)$ from site J, and $(2S)(2S)\times(2S-1)$ from site i.

Although Eqs. (23) or (25) are nominally in the form of a Wick's theorem for spin operators, the theory is empty until a simple and tractable prescription for the evaluation of the u factor is demonstrated. We shall indicate this prescription in diagrammatic terms.

To represent the chronological product diagrammatically we represent time along the horizontal axis (increasing from right to left). Different crystal sites are distinguished by different vertical positions in our diagrams. The propagator $\langle 0|Pv_iv_j^\dagger|0\rangle$ is represented by a directed solid line, from the space-time point j (designated by a cross) to the space-time point i (designated by a circle). Since

$$\langle 0|Pv_iv_j^\dagger|0\rangle=e^{-i\omega_{0i}(t_i-t_j)}\theta(t_i-t_j)\delta_{i,j}\,, \tag{26}$$

we see that all such solid lines must proceed to the left and must be horizontal. Consequently, the chronological product $\mathcal{G}$ is represented by a set of horizontal lines, some at the same site (same vertical position) and some possibly at different sites (different vertical positions). Those at a single site may or may not overlap. Such a diagram is shown in Fig. 1.

The u factor associated with a given diagram can be read directly as follows: We just note that the order of the operators in the u factor is completely determined by the crosses and circles associated with the v's; reading from right to left each cross implies a u operator and each circle represents a $u^\dagger$ operator. Then the u factor is obtained by associating to each cross in the diagram a factor $(2S-n^\times+n^\circ)$, where $n^\times$ is the number of crosses and n° is the number of circles to the right of (and at the same site as) the given cross. Thus the u factor in Fig. 1 is $(2S)^4(2S-1)$.

Unfortunately the u factor depends on the relative time sequence of the v-particle propagators. In the applications of the Wick theorem we generally integrate over all internal times, so that the u factor changes discontinuously in the course of the integration. The essence of our method lies in the manner by which these variations in the u factor are made manageable.

Consider the diagram of Fig. 2(a). The u factor of this diagram is $2S(2S-1)=(2S)^2-2S$. We now represent each term in this expression by a separate "new-type" diagram. The term $(2S)^2$ will be associated with the diagram (b), where we now associate the factor $2S$ with

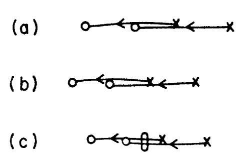

FIG. 2. The diagram (a) is replaced by the sum of two "new-type" diagrams (b) and (c). The u factor of (a) is $2S(2S-1)=(2S)^2-2S$. The two terms in this u factor are associated with diagrams (b) and (c), respectively.

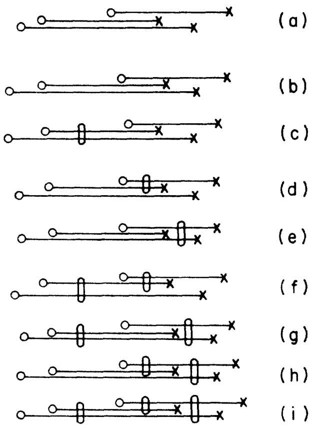

FIG. 3. The old-type diagram (a) had the u factor $(2S)(2S-1)(2S-2)=(2S)^3-3(2S)^2+2(2S)$. Diagram (b) contributes $(2S)^3$. Diagrams (c)–(e) are each negative (one lock) and consist of two disjoint parts; they contribute $-3(2S)^2$. Diagrams (f)–(h) are positive (-1 for each lock) and contain a single disjoint part; they contribute $3(2S)$. Finally, (i) contributes $-(2S)$.

each line in the diagram, independently of the sequence of crosses and circles; that is, the time indices in Fig. 2(b) are free. The correction diagram (c) is said to be "locked", implying that the time indices are constrained to such values that the two lines remain half-overlapping. The factor (-1) is associated with the "lock" in the diagram and the factor $(2S)$ is obtained by associating a factor $2S$ with each connected set of lines, (i.e., with each set which is connected together by locks). For Fig. 2(b) each separate line is such a set, so each line separately carried its own factor of $(2S)$. In Fig. 2(c) the two locked lines form a single set and contribute only one factor $(2S)$.

One more specific example, which should make the procedure clear, is given in Fig. 3.

The general decomposition of old-type diagrams into new-type diagrams is discussed in the Appendix. We here simply summarize the results.

A chronological product of spin operators can be replaced by a set of v-particle propagators satisfying the usual form of Wick's theorem. However, each conventional diagram (with free-time indices) is to be supplemented by correction diagrams, in which one or more half-overlapping or full-overlapping lines are "locked together," restricting the range of the time indices. In addition, each diagram carries a factor (-1) for each lock and a factor $(2S)$ for each connected set of lines (lines connected by locks).

The theorem proved above referred to chronological products containing only S_i^+ and S_i^- operators [Eq. (20)]. Introduction of S_i^z operators would introduce factors of $(S-v_i^\dagger v_i)$ into Eq. (21); the S term reduces to the case already considered. The $v_i^\dagger v_i$ term then changes the v factor in Eq. (22) *without altering the u factor*. In the Wick representation of the v factor the operators $v_i^\dagger v_i$ will introduce a "double vertex" such as is shown in Fig. 4. For the purpose of attaching locks, then, we merely ignore such double vertices, considering the two propagators joined at this vertex as if they were a single propagator. Unlike single vertices, locks impose no constraints on double vertices. With this addition to our previous result the form of Wick's theorem is completely general, for arbitrary chronological products of spin operators.

FIG. 4. A "double" vertex arising from an S_i^z operator.

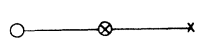

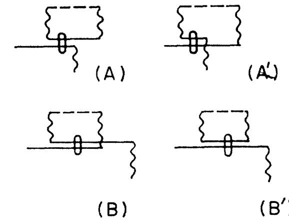

FIG. 5. Relationship of the locked half-overlapping diagrams and the locked full-overlapping diagrams.

3. THE LINKED-DIAGRAM THEOREM: SIMPLE ANTIFERROMAGNETS

The Goldstone linked-diagram theorem is now quite straightforward, but it is most conveniently discussed in terms of a specific Hamiltonian. For this purpose we consider an isotropic Heisenberg antiferromagnet with two interpenetrating sublattices such that the nearest neighbors of a spin on one sublattice all lie on the other sublattice. For the "down" sublattice (designated by Roman indices) we make the coupled-boson substitution of Eqs. (1)–(3), but for the "up" sublattice (designated by Greek indices) it is convenient to invert the role of the two types of bosons:

$$S_\alpha^- = v_\alpha^\dagger u_\alpha, \quad S_\alpha^+ = u_\alpha^\dagger v_\alpha, \tag{27}$$

$$S_\alpha^z = S - v_\alpha^\dagger v_\alpha. \tag{28}$$

The ground state $|0\rangle$ is then

$$|0\rangle = \prod_i \prod_\alpha [(2S)!]^{-1} (u_i^\dagger)^{2S} (u_\alpha^\dagger)^{2S} \| 0\rangle. \tag{29}$$

The Hamiltonian is $\mathcal{H}_0 + V$, where

$$\mathcal{H}_0 = E_0 + \omega_0 \sum_i v_i^\dagger v_i + \omega_0 \sum_\alpha v_\alpha^\dagger v_\alpha, \tag{30}$$

in which we note that the last term has been rendered positive by the inversion of the roles of u-particles and v-particles on the up sublattice. Also,

$$V = \sum_{i,\alpha} \{ J_{i\alpha} (v_i^\dagger v_\alpha^\dagger u_i u_\alpha + v_i v_\alpha u_i^\dagger u_\alpha^\dagger) - 2J_{i\alpha} v_i^\dagger v_i v_\alpha^\dagger v_\alpha \}. \tag{31}$$

Consider now the Green's function

$$G(l,m) = -i(0|P\tilde{S}_l^- \tilde{S}_m^+|0) \tag{32}$$

$$= -i\langle 0|P v_l v_m^\dagger u_l^\dagger u_m \mathcal{S}(\infty)|0\rangle / \langle 0|\mathcal{S}(\infty)|0\rangle, \tag{33}$$

where the spin operators in (32) are in Heisenberg representation, and $|0)$ denotes the true ground state. Equation (33) has been transformed to interaction representation in the usual way, assuming the "adiabatic turning-on theorem."[7] Series expansion of $\mathcal{S}(\infty)$ now generates a series of terms in both numerator and denominator, and each term contains a chronological product of the type discussed in the preceding section.

The unperturbed propagators on down and up sublattices will be distinguished by representing them with solid and dashed horizontal lines, respectively. Each proceeds to the left, from a cross to a circle. The cross on an up site is connected by a vertical interaction (wavy) line to a cross on a neighboring down site, and similarly for circles. Double vertices (or, better, "longitudinal vertices") of the type shown in Fig. 4 are similarly connected by vertical interaction lines. The contribution of each diagram is calculated by the following rules: (1) To each horizonal solid or dashed line associate an unperturbed propagator, of value $-i\exp\{-i\omega_0(t_{\text{final}}-t_{\text{initial}})\}$. (2) To each vertical interaction line which connects two crosses or two circles, associate the factor J. (3) To each vertical interaction line which connects two longitudinal vertices, associate the factor $-2J$. (4) To each lock, associate the factor (-1). (5) To each set of horizontal lines which are interconnected by locks, or by "double vertices" (cf., Fig. 4), associate the factor $2S$. Finally, draw all possible diagrams [those in the numerator of Eq. (33) have one incoming line from the right and one outgoing line to the left, whereas those in the denominator consist only of closed loops], integrate over all internal time coordinates (subject to the constraints imposed by the locks), sum over all internal sites, and add the contributions of all diagrams.

Clearly the diagrams of the numerator can be composed of two or more unconnected parts. Such parts are entirely independent, this independence being the very purpose of our "lock" device (i.e., the elimination of "excluded volume" restrictions on site sums). Consequently the numerator factors into a product of the loop diagrams of the denominator times the sum of connected diagrams joined to the external lines. Cancellation gives the Goldstone result:

$$G(l,m)=-i\langle 0|Pv_l v_m{}^\dagger u_l{}^\dagger u_m \mathcal{S}(\infty)|0\rangle_{\text{connected}}, \quad (34)$$

with the diagram conventions discussed above. In particular it should be recalled that only v-particle lines appear in the diagrams, the u-particles being accounted for implicitly by rules (4) and (5) above.

4. ANTIFERROMAGNETIC SPIN WAVES

As an illustration of the application of the above theorems we briefly summarize the theory of antiferromagnetic spin waves given in I, generalizing it to arbitrary spin.

The simplest diagrams contributing to $G(l,m)$ are the chain diagrams, containing no longitudinal interactions and no locks (Fig. 5 of I). Summation of these diagrams trivially yields Anderson's simple spin-wave theory (Sec. 6 of I). The simplest correction diagrams are those with a single longitudinal interaction line or a single lock. As shown in I, and as we shall discuss below, these simplest correction diagrams are also of lowest order in the expansion parameter $1/(2zS)$.

The lock diagrams appearing in the present theory may involve either full-overlapping lines or half-overlapping lines. This is in contrast to I, in which only half-overlapping locked lines were considered. However, it is immediately apparent that for any locked half-overlapping diagram there exists a locked full-overlapping diagram and vice versa. In fact one need only to change the interconnection of the four vertices of the two locked propagators to convert one diagram to the other, as indicated in Fig. 5. Furthermore, the contribution of a locked full-overlapping diagram is easily seen to be identical to that of its corresponding lock half-overlapping diagram. This observation permitted us to consider only half-overlapping lock diagrams in I, doubling their contribution to account implicitly for the full-overlapping correction diagrams. In the discussion below we shall again make explicit reference only to half-overlapping correction diagrams. The summation procedure of correction diagrams is then identical to that given in I.

It will be recalled that the first order correction diagrams could be summed into four distinct types of self-energy corrections, designated Σ_1, Σ_2, Σ_3, Σ_4. Consider the loop-type self-energy Σ_1 (Fig. 8 of I). The upper Green's function in the loop now carries an additional factor of $2S$; the lower Green's function does not, as it is connected to the remainder of the diagram. Thus the second of Eqs. (7.4) in I must be multiplied by $2S$. In addition ω_0 must now be interpreted as

$$\omega_0=2SJ(0). \quad (35)$$

In this way, Eq. (7.7) of I becomes

$$\Sigma_1=\omega_0/2S[2\delta S_0{}^z+\Delta]. \quad (36)$$

Similarly the expressions given in I for Σ_2, Σ_3 and Σ_4 must each now be divided by $2S$.

$$\Sigma_2=-(1/2S)[2\delta S_0{}^z], \quad (37)$$

$$\Sigma_3=\omega_0\Sigma_2, \quad (38)$$

$$\Sigma_4=\Sigma_1/\omega_0. \quad (39)$$

As before, the sum $(\Sigma_1+\Sigma_3)$ renormalizes the unperturbed Green's functions, shifting their poles from ω_0 to $\omega_0[1+\Delta/2S]$. The exchange interaction is renormalized by $(\Sigma_2+\Sigma_4)$, so that the effective interaction is $J(\mathbf{k})[1+(\Delta/2S)]$. If these renormalized unperturbed Green's functions and effective interactions are in-

[7] See for example, A. A. Abrikosov, L. P. Gorkov, and Z. E. Dzyaloshinski, *Methods of Quantum Field Theory in Statistical Physics* (Prentice-Hall Publishers Inc., Englewood Cliffs, New Jersey, 1963), Chap. 2.

serted in the simple spin-wave result, one obtains [as in Eqs. (7.18)-(7.20) of I]

$$\epsilon^{(1)}(\mathbf{k})=[1+(\Delta/2S)]J(0)(1-\gamma_\kappa^2)^{1/2}, \tag{40}$$

which is Oguchi's result.

We consequently observe that the quantities Δ and δS_0^z, which are of order $1/z$ and which constitute the expansion parameters of I, are now replaced by $\Delta/2S$ and $\delta S_0^z/(2S)$. That is, the expansion parameter for general S is $(2zS)^{-1}$.

APPENDIX

We here demonstrate the theorem given in the next-to-last paragraph of Sec. 2. The content of the theorem is that the u factor of any old-type diagram is reproduced by the sum of the corresponding new-type diagrams (with all possible lockings), where each lock carries the weight factor (-1) and each connected set of lines (lines connected by locks) carries a factor $(2S)$.

Since the u factor of any diagram is the product of the u factor for each site we restrict our attention to the lines on a single site. The u factor is the product of factors $(2S-n^\times+n^\circ)$, where $n^\times$ is the number of crosses and n° is the number of circles to the right of each cross. The theorem in question is equivalent to the statement that this u factor can be written in the form

$$\begin{aligned}u_{12\cdots\alpha}=&(2S)^\alpha N_0{}^0-(2S)^{\alpha-1}N_1{}^1+(2S)^{\alpha-2}(N_2{}^2-N_2{}^3)\\&-(2S)^{\alpha-3}(N_3{}^3-N_3{}^4+N_3{}^5-N_3{}^6)+\cdots\\&+(-1)^{\alpha-1}(2S)(N_{\alpha-1}{}^{\alpha-1}-N_{\alpha-1}{}^{\alpha}+\cdots\pm N_{\alpha-1}{}^{\alpha(\alpha-1)/2}),\end{aligned} \tag{A1}$$

where α is the number of lines on the given site, and $N_{\alpha-D}{}^l$ is the number of single-site diagrams with l locks and with D connected sets of lines which can be constructed. Although this theorem is a fairly evident generalization which can be drawn from inspection of individual cases (compare, for instance, with Figs. 2 and 3), we do not have a general and formal proof at this time. Several special cases lend support to the general theorem, and we briefly note these.

For the special case of $S=\frac{1}{2}$ the theorem (A1) is quite easy to prove. The u factor is clearly unity if no lines overlap, and is zero otherwise. Consider, now the right-hand member of Eq. (A1), which reduces to

$$\begin{aligned}u_{12\cdots\alpha}&=N_0{}^0-N_1{}^1+N_2{}^2-N_2{}^3\\&\qquad-N_3{}^3+N_3{}^4-N_3{}^5+N_3{}^6-\cdots\\&=N_0{}^0-N_1{}^1+N_2{}^2\\&\qquad-(N_2{}^3+N_3{}^3)+(N_3{}^4+N_4{}^4)+\cdots.\end{aligned} \tag{A2}$$

But $(N_2{}^3+N_3{}^3)$ is the total number of ways of assigning 3 locks, and similarly for the higher order terms. Let $l_{\max}$ denote the maximum number of locks which could be distributed on the given configuration of lines. Then clearly $(N_2{}^3+N_3{}^3)$ is simply the binomial coefficient

$$\binom{l_{\max}}{3}.$$

Thus

$$u_{12\cdots\alpha}=\binom{l_{\max}}{0}-\binom{l_{\max}}{1}+\binom{l_{\max}}{2}-\cdots \tag{A3}$$

$$\begin{aligned}&=(1-1)^{l_{\max}}, &&\text{if}\quad l_{\max}\neq 0;\\&=1, &&\text{if}\quad l_{\max}=0,\end{aligned} \tag{A4}$$

in agreement with the known value of the u factor.

Another special case in which a proof is easily given (for general S) is that a set of p lines every one of which overlaps every other one. Then a lock can be placed between any pair of lines. The problem is now very similar to a conventional linear graph problem in statistical mechanics.[8] The lines and locks in our diagrams are analogous to the points and the bonds in the linear graph theory.

Consider the following generating functions[8]:

$$f(x)\equiv\sum_{p=1}^{\infty}\Big(\sum_{l=p-1}^{C_2{}^p}n_p{}^l(-1)^l\Big)\frac{x^p}{p!}, \tag{A5}$$

and

$$F(x)\equiv\sum_{p=1}^{\infty}\Big(\sum_{l=0}^{C_2{}^p}U_p{}^l(-1)^l\Big)\frac{x^p}{p!}, \tag{A6}$$

where $n_p{}^l$ is the number of connected diagrams which can be obtained with l locks in the set of p lines and $C_2{}^p\equiv\binom{p}{2}$. Similarly $U_p{}^l$ is the total number of diagrams (connected and disconnected) which can be obtained with l locks in the set of p lines.

The restriction $l\geq p-1$ in Eq. (A5) follows from the condition that the diagrams in (A5) must be connected.

From the "product theorem" it follows that[8]

$$1+F(x)=e^{f(x)}. \tag{A7}$$

We can calculate $F(x)$ easily, for

$$\sum_{l=0}^{C_2{}^p}U_p{}^l(-1)^l=\sum_{l=0}^{C_2{}^p}\binom{C_2{}^p}{l}(-1)^l \tag{A8}$$

$$\begin{aligned}&=(1-1)^{C_2{}^p}, &&\text{if}\quad p\neq 1;\\&=1 &&\text{if}\quad p=1,\end{aligned} \tag{A9}$$

whence

$$F(x)=x, \tag{A10}$$

and

$$f(x)=\ln(1+x). \tag{A11}$$

Returning to the generating functions (A5) and (A6) we note that they associate a weight of $(-1)^l$ to each diagram. We are interested in associating an additional factor $2S$ to each connected cluster. Denoting the generating functions with this additional weighting by a tilde, it is clear that

$$\tilde{f}(x)=2Sf(x), \tag{A12}$$

[8] G. E. Uhlenbeck and G. W. Ford, in *Studies in Statistical Mechanics*, edited by J. DeBoer and G. E. Uhlenbeck (North-Holland Publishing Company, Amsterdam, 1962).

since the diagrams contributing to $f(x)$ are composed of only a single connected cluster. Then,

$$1+\tilde{F}(x)=\exp[\tilde{f}(x)]=(1+x)^{2S}. \tag{A13}$$

But

$$\tilde{F}(x)\equiv\sum_{p=1}^{\infty}F_p\frac{x^p}{p!}, \tag{A14}$$

where F_p is the weight factor associated with the complete set of diagrams on p lines. From (A13) and (A14) we find

$$F_p=2S(2S-1)(2S-2)\cdots(2S-p+1), \tag{A15}$$

which is just the proper weight factor previously designated by $u_{12\cdots p}$.

PHYSICAL REVIEW VOLUME 148, NUMBER 1 5 AUGUST 1966

Broadening of Paramagnetic-Resonance Lines by Internal Electric Fields

W. B. MIMS AND R. GILLEN
Bell Telephone Laboratories, New York, New York
(Received 21 March 1966)

The paramagnetic-resonance linewidth for ions in axial sites in $CaWO_4$ has been measured with **H** in the azimuthal plane. Large variations are observed, the maximum widths occurring at orientations where the shift of the resonance in an applied electric field is greatest. It is concluded that electric fields of the order of 50 kV/cm are seen at the paramagnetic centers, and that these fields are caused by randomly distributed defects in the crystal lattice. The line shape has been calculated and compared with experiment. Agreement is satisfactory and suggests that the measurement of resonance linewidths might be used to obtain accurate measurements of defect concentration in suitable ionic crystals. The effects of mechanical strains, and the role of internal electric fields in determining optical properties are briefly discussed.

It is commonly found that the width of paramagnetic-resonance lines cannot be reduced indefinitely by reducing the concentration of magnetic ions. In cases where the host crystal contains nuclei with large moments the residual linewidth at high dilutions can often be attributed to the local magnteic fields generated by randomly oriented nuclei surrounding the ion, but there remain many instances for which the linewidth cannot be explained by any form of magnetic interaction. Randomly distributed strains, and a mosaic structure in the crystal have been invoked as possible causes of this nonmagnetic broadening.[1–4] It is our purpose to show here that additional broadening can be caused by the electric fields which are generated inside the crystal by randomly distributed charge defects. If the paramagnetic ion is at a site which lacks inversion symmetry these fields give rise to proportional shifts in frequency, and they may, in some cases, be the paramount factor in determining the width of the resonance line.

We begin with the experimental evidence. Figure 1 shows the full width at half-height for the resonance line of Ce^{3+} in a $CaWO_4$ lattice as a function of crystal orientation when the Zeeman field H_0 is rotated in the plane perpendicular to the c axis. The ground state of Ce^{3+} is a Kramers doublet and its resonance is characterized by two g values, $g_{\parallel}=2.92$ along the c axis, and $g_{\perp}=1.43$ in the plane perpendicular to it. The resonance energy is therefore constant when H_0 is rotated in the ab plane, and it is only changed to the second order by slight rotations out of the plane such as those which might occur if the crystal had a mosaic structure. We observe however that the linewidth changes by a factor 5, reaching a maximum every 90°, and passing through a minimum at an angle of 8° with respect to the a and b axes. The linewidth curve strongly resembles the curve obtained earlier for the linear electric shift of Ce^{3+} in $CaWO_4$, and passes through a minimum at the angle where the electric shift is zero.[5,6] To facilitate the comparison and help in establishing the magnitudes involved, the electric field shift for a field along the c axis of 100 kV/cm is plotted as a function of angle φ on the same graph. Similar results were obtained with Er and Mn dopings, and the corresponding curves are shown in Figs. 2 and 3. (It should be noted that electric fields applied along the a or b axes give no shifts in these materials when the resonance is observed in the ab plane.)

The graphs in Figs. 1–3 suggest at once that there are internal electric fields of the order of 50 kV/cm and that these fields are responsible for the greater part of the observed line broadening. Magnetic broadening can be almost entirely ignored for these samples. The

[1] D. Shaltiel and W. Low, Phys. Rev. **124**, 1062 (1961).
[2] Elsa Feher, Phys. Rev. **136**, A145 (1964).
[3] P. L. Scott, H. J. Stapleton, and C. Wainstein, Phys. Rev. **137**, A71 (1965).
[4] R. F. Wenzel and Y. W. Kim, Phys. Rev. **140**, A1592 (1965).
[5] W. B. Mims, Phys. Rev. **140**, A541 (1965).
[6] In order to make this comparison independent of errors in the mounting of the crystal, electric field shifts and linewidths were measured at the same time. A microwave resonance frequency 9.42 Gc/sec. was used in these experiments.